Food Hydrocolloids 167 (2025) 111467

Contents lists available at ScienceDirect

Food Hydrocolloids

journal homepage: www.elsevier.com/locate/foodhyd

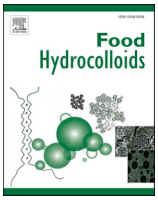

Oil-water interfacial and emulsifying properties of lupin protein and lupin protein-pectin mixtures at neutral and acidic pH conditions

Xingfa Ma *, Mehdi Habibi, Leonard M.C. Sagis

Laboratory of Physics and Physical Chemistry of Foods, Wageningen University, Bornse Weilanden 9, 6708 WG, Wageningen, the Netherlands

ARTICLE INFO

Keywords:
Lupin protein
Lupin-pectin mixtures
Neutral and acidic pH
Interfacial rheology
General stress decomposition
Emulsion properties

ABSTRACT

Lupin proteins have high nutritional value and can be used to form foams, emulsions, and gels. However, their functionality becomes poor at acidic pH due to reduced protein solubility. Protein solubility and functionality at acidic pH can be improved by adding polysaccharides. In this study, we compared the oil-water interfacial and emulsifying properties of lupin protein isolates (LPI) and LPI-pectin mixtures at pH 7.0, pH 6.0, pH 4.0, and pH 3.5. Overall, LPI-pectin complexes at pH 4.0 and 3.5 showed better interfacial properties and emulsion stabilization than LPI at pH 4.0 and 3.5, while LPI-pectin mixtures at pH 7.0 and 6.0 displayed comparable interfacial and emulsion properties as LPI at 7.0 and 6.0. We observed that LPI at pH 4.0 and pH 3.5 adsorbed faster to the oil-water interface than LPI-pectin complexes at pH 4.0 and 3.5, due to smaller particle sizes of LPI, while LPI and LPI-pectin mixtures at pH 7.0 and 6.0 showed comparable adsorption rates to the oil-water interface. The LPI-pectin mixtures at pH 6.0 and 7.0 formed weak oil-water interfaces, with a stiffness comparable to LPI at these pH values. While at pH 3.5 and 4.0 LPI-pectin complexes formed stiffer oil-water interfaces than LPI. As a result, LPI-pectin complexes at pH 4.0 and 3.5 showed better emulsifying properties and emulsion stability against coalescence during high-shear mixing. The emulsion stabilized with LPI-pectin complex at pH 3.5 showed more extensive flocculation than the complex at pH 4.0, due to the reduced charges of the complex at pH 3.5 and depletion flocculation induced by non-adsorbed complexes. Our study reveals that the complexation of proteins with pectin at acidic pH could be a useful way to improve the oil-water interfacial and emulsifying properties of proteins at acidic pH, and could potentially be used in the food industry to develop plant protein-based emulsion products.

1. Introduction

Lupins (*Lupinus* L) are cultivated in Australian and Mediterranean regions and have attracted increasing attention from the food industry due to their high protein content and health benefits (Arnoldi et al., 2015; Van de Noort, 2024). Lupin seeds, such as *L. angustifolius*, contain 33–46 % of proteins, 6.8–8.1 % of fat, 14–36 % of fiber, 3.4–3.9 % of ash, and 4.8–7.9 % of carbohydrates (Bähr et al., 2014; Chin et al., 2019; Sujak et al., 2006). Lupin proteins can be extracted from the seeds and applied as plant-based functional ingredients for potential use in food products (Boukid & Pasqualone, 2022). According to previous studies, lupin proteins mainly consist of α-, β-, γ-, and δ-conglutin (Duranti et al., 2008; Muranyi et al., 2016; Shrestha, van't Hag, Haritos, & Dhital, 2021). Of these components, α- and β-conglutin are the main storage proteins with 80–90 % of total protein contents, while γ- and δ-conglutin are the minor fractions with around 4–5 % and 10–12 % of the total protein contents (Melo et al., 1994). Currently, lupin proteins have been used in food industry, such as spaghetti (Doxastakis et al., 2007), cookies (Mota, Lima, B. Ferreira, & Raymundo, 2020), bread (Paraskevopoulou et al., 2010), yogurt (Hickisch et al., 2016), and meat products (Drakos et al., 2007). However, the application of lupin proteins is still limited in acidic food products due to the reduced protein solubility at acidic pH.

Several studies have investigated the emulsifying properties of lupin proteins at different pH (Albe-Slabi et al., 2022; Chukwuejim & Aluko, 2024; Jayasena et al., 2010; Opazo-Navarrete et al., 2022; Raymundo et al., 2000). It was found that lupin proteins at pH 7 formed emulsions with smaller droplet sizes and lower degree of droplet coalescence than those at pH 3 and pH 5 (Chukwuejim & Aluko, 2024). Another study by Albe-Slabi et al. (2022) also showed that lupin proteins at pH 2 had lower emulsifying capacity than those at pH 7. The poor emulsifying properties of lupin proteins at acidic pH were mainly attributed to the reduced net charges of protein molecules resulting in droplet

* Corresponding author.
E-mail address: xingfa.ma@wur.nl (X. Ma).

https://doi.org/10.1016/j.foodhyd.2025.111467
Received 19 February 2025; Received in revised form 17 April 2025; Accepted 21 April 2025
Available online 21 April 2025

flocculation. Additionally, a recent review has shown that pectin molecules by themselves have poor interfacial activity, but this can be improved by means of chemical modifications, such as acid/alkali hydrolysis, enzymatic modifications, Mallard reactions, chemical cross-linking, and electrostatic bonding (Niu et al., 2025). To improve the emulsifying properties of proteins at acidic pH, it was suggested to use polysaccharides to form electrostatic complexes with proteins, which can provide electrostatic and steric repulsions to stabilize emulsions at acidic pH (Ma & Chatterton, 2021). In the past few years, the emulsifying properties of protein-polysaccharide complexes have been extensively reported (Dalev & Simeonova, 1995; Girard et al., 2002; Kato et al., 1989; Lopes-da-Silva & Monteiro, 2019; Wang et al., 2019; Zhao et al., 2022). Only a few studies discussed the oil-water interfacial properties of protein-polysaccharide complexes (Gharsallaoui et al., 2010; Li et al., 2016; Wang et al., 2020; Yang & Xiang, 2022; Zhang et al., 2020). As a result, details on the exact mechanisms by which protein-polysaccharide mixtures stabilize oil-water interfaces, and how these are affected by pH, are often unknown.

In a previous study, lupin proteins showed better foaming functionality at pH 3.5 and 4.0 than those at pH 6.0 and 7.0; however, the lower solubility of proteins at acidic pH (~44 %) could limit their application in the food industry (Ma et al., 2024a). Pectin was used to increase the solubility of lupin proteins at acidic pH through protein-pectin electrostatic complexation, which also improved the foaming functionality of lupin proteins at acidic pH (Ma et al., 2024b). In the current study, the focus will be on the oil-water interfacial and emulsifying properties of lupin protein-pectin mixtures at pH 3.5–7.0, compared to pure lupin proteins at the same pH range. We first investigated the oil-water interfacial properties (e.g., interfacial adsorption behavior and interfacial rheology) of lupin protein-pectin mixtures (1:1 ratio) and pure lupin proteins at pH 3.5–7.0. Subsequently, we studied the emulsion properties (emulsifying properties and emulsion stability under turbulent mixing) for the mixtures and pure LPI, which were then linked to the interfacial properties. This study provides a more comprehensive understanding of the oil-water interfacial and emulsifying properties of lupin protein-pectin mixtures and pure lupin proteins at different pH, which could promote their applications in the food industry.

2. Materials and methods

2.1. Materials

Lupin seeds were purchased from Kamelur (Germany), pectin (GENU®, 45CS) was received from CPKelco (Atlanta, GA) with a degree of esterification of 38 %, and all other chemicals were received from Sigma-Aldrich (USA). All solutions in this study were prepared in MilliQ water.

2.2. Extraction of lupin proteins

The extraction of lupin protein isolates (LPI) was based on our previous study (Ma et al., 2024a). Briefly, lupin flour was first prepared by dehulling and milling seeds, using a laboratory scale dehuller (Satake Corporation, Japan), and a multimill (Hosokawa-Alpine, Augsburg, Germany) with a ZPS50 configuration, followed by defatting the flour using hexane. The defatted flour was then dispersed in MiliQ water at pH 9 and centrifuged at 36,000 g for 10 min to obtain the supernatant. The pH of the supernatant was then adjusted to 4.6, and the sample was centrifuged at 36,000 g for 5 min to collect the pellet containing the globulin fractions, while the supernatant containing albumins was discarded. The pellets were redispersed in MiliQ water, and then the pH was adjusted to 7.2. Lastly, the redispersed dispersions were dialyzed over 12 kDa cut-off membranes against MiliQ water at 4 °C for 72 h, and then freeze-dried before further use. The protein content in the resultant protein isolate was 81.7 ± 3.8 % based on a conversion factor of 5.7. The protein characterizations, including size, charge, and surface hydrophobicity, can be found in Fig. S1.

2.3. Preparation of sample solutions

LPI solutions at 0.1 wt% concentration were prepared at pH 7.0 (denoted as LPI-7), pH 6.0 (denoted as LPI-6), pH 4.0 (denoted as LPI-4), and pH 3.5 (denoted as LPI-3.5), based on soluble protein content, by dispersing protein powder in 20 mM pH 7 phosphate buffer, 20 mM pH 6 phosphate buffer, 20 mM pH 4 acetate buffer, and 20 mM pH 3.5 citrate buffer, respectively. As to the preparation of LPI-pectin mixtures, LPI and pectin powders were dispersed in MiliQ water at a concentration of 0.2 wt%. Afterwards, the mixed solutions were prepared by mixing LPI and pectin solutions at a 1:1 ratio, and then diluting the mixtures with 40 mM pH 7 phosphate buffer, 40 mM pH 6 phosphate buffer, 40 mM pH 4 acetate buffer, and 40 mM pH 3.5 citrate buffer, respectively, to reach a final total concentration of 0.1 wt% of LPI-pectin mixtures. All protein and pectin solutions were stirred for 4 h at room temperature and then kept overnight at 4 °C before further use. Those protein solutions were also passed through 0.45 μm syringe filters to remove any insoluble particles.

2.4. Oil-water interfacial adsorption kinetics

The oil-water interfacial adsorption behavior of LPI and LPI-pectin mixtures was measured by an automated drop tensiometer (Teclis, France). A rising droplet (MCT oil) with a 30 mm^2 area was generated at the tip of the G18 needle in the 0.1 wt% concentration of LPI or LPI-pectin mixed solutions. Subsequently, the droplet was equilibrated for 3 h with continuous monitoring of the interfacial tension. The interfacial pressure (Π) was calculated as $\Pi(t) = \gamma_0 - \gamma_{(t)}$, where γ_0 is the interfacial tension of the clean oil-water interface and $\gamma_{(t)}$ is the interfacial tension in real-time. These measurements were performed at least in triplicate at 20 °C.

2.5. Interfacial shear rheology

The interfacial shear rheology of LPI and LPI-pectin mixtures was measured by a stress-controlled MCR 302e rheometer (Anton Paar, Graz, Austria) coupled with a double-wall ring (DWR) geometry. Briefly, 15 ml of 0.1 wt% protein solutions were injected into the bottom of the Teflon double wall trough, and the DWR geometry was positioned at the liquid interface. Subsequently, 7.5 ml of MCT oil was injected on top of the protein solutions, which created oil-water interfaces. Then, a time sweep was initially performed at a strain of 0.1 % and frequency of 0.1 Hz during 3 h of adsorption. A frequency sweep was then conducted from 0.01 Hz to 2 Hz and at a fixed strain of 1 %. The data from the frequency sweep were used to fit a power-law model ($G' = \omega^n$) to obtain the exponent n. Lastly, a strain sweep was performed using large amplitude oscillatory shear (SAOS) and large amplitude oscillatory shear (LAOS) at strains from 0.01 % to 100 % and a fixed frequency of 0.1 Hz. The nonlinearities in the response to the strain sweeps were further analyzed by Lissajous plots and by calculating the energy dissipation ratio (φ). The energy dissipation ratio is defined as $\varphi = \frac{\pi G'' \gamma_0}{4\sigma_{max}}$ according to Ewoldt et al. (2008), where G″ is the loss modulus, γ_0 is the strain amplitude, and σ_{max} is the maximum stress.

2.6. Interfacial dilatational rheology

The interfacial dilatational rheology of LPI and LPI-pectin mixtures was measured by an automatic drop tensiometer (Teclis, France) according to Section 2.4. During 3 h of adsorption, a time sweep was first conducted at an amplitude of 3 % and a frequency of 0.02 Hz. After 3 h of adsorption, a frequency sweep was performed at a fixed amplitude of 3 % and a frequency ranging from 0.005 Hz to 0.01 Hz. The data from

the frequency sweep were used to fit a power law model ($E_d' \sim \omega^m$) to obtain the exponent *m*. Afterwards, an amplitude sweep was conducted using small amplitude oscillatory dilatation (SAOD) and large amplitude oscillatory dilatation (LAOD) at amplitudes from 3 % to 30 % and a fixed frequency of 0.02 Hz. The data from amplitude sweeps were used to calculate the first harmonic moduli (E_d' and E_d''), and the full surface stress signal, including contributions from higher harmonics, was further used to construct Lissajous plots, which were analyzed using the general stress decomposition method (GSD) (de Groot, Yang, & Sagis, 2023b).

2.7. Emulsion properties

2.7.1. Preparation of emulsions

Stock solutions of LPI and LPI-pectin were prepared at a total concentration of 0.1 wt% and 0.5 wt% at pH 7, pH 6, pH 4, and pH 3.5, in the corresponding buffer as mentioned in Section 2.3. Coarse emulsions were first prepared by blending the LPI and LPI-pectin solutions with MCT oil at a ratio of 9:1 (w/w) using a high-shear blender (UltraTurrax, IKA, Staufen, Germany) at 12000 rpm for 2 min. Afterwards, the coarse emulsions were passed through a GEA high-pressure homogenizer (Niro Soavi NS 1001L, Parma, Italy) at room temperature at 180 bar for 10 cycles. The emulsions were stored at 4 °C overnight before further analysis.

2.7.2. Zeta potential measurement

The zeta potential of fresh emulsions was measured with a ZetaSizer Nano ZS (Malvern Instruments, UK). Before measurement, the emulsions were diluted 200 times using their corresponding buffers mentioned in Section 2.3. The refractive index of MCT oil and continuous phase was set at 1.450 and 1.330, respectively.

2.7.3. Determination of droplet size

The droplet size distribution of the freshly prepared emulsions was measured by a Mastersizer 3000 (Malvern Panalytical, UK). The refractive index used for MCT oil and continuous phase were 1.450 and 1.330, respectively. To check for droplet flocculation, the emulsions were mixed with 1 wt% SDS solution at a 1:1 ratio before the droplet size measurement.

2.7.4. Stability of emulsions against high flow rate

To measure the stability of the emulsions under flow conditions, the 0.5 wt% emulsions were subjected to a high intensity mixing treatment using an UltraTurrax (IKA, Staufen, Germany) at speeds of 5000 rpm, 10000 rpm, and 15000 rpm for 1 min. Afterwards, the emulsions were mixed with 1 wt% SDS solution and then the droplet size was measured according to the same procedures in Section 2.7.3.

2.8. Statistical analysis

One-way analysis of variance (ANOVA) of the data was conducted by OriginPro 2021. The means comparison among samples was conducted by Tukey's test using a significant level of 0.05.

3. Results and discussion

3.1. Oil-water interfacial properties of LPI and LPI-pectin mixtures

3.1.1. Adsorption behavior

The oil-water interfacial adsorption behavior of lupin protein at pH 7 (LPI-7), pH 6 (LPI-6), pH 4 (LPI-4), and pH 3.5 (LPI-3.5) and lupin protein-pectin mixtures at pH 7 (LPI-pectin-7), pH 6 (LPI-pectin-6), pH 4 (LPI-pectin-4), and pH 3.5 (LPI-pectin-3.5) during 3 h of adsorption is shown in Fig. 1A–C and Fig. 1D–F, respectively. It should be noted that LPI and pectin at pH 7 and 6 were co-solubilized in the bulk phase due to strong electrostatic repulsions, while LPI-pectin complexes were formed at pH 4 and 3.5 due to electrostatic interactions (Ma et al., 2024b). Therefore, we classify LPI-pectin-7 and LPI-pectin-6 as co-solubilized mixtures, while we regard LPI-pectin-4 and LPI-pectin-3.5 as electrostatic complexes.

LPI showed a higher interfacial pressure at pH 4 (5.6 mN/m) and pH 3.5 (6.6 mN/m) than LPI-pectin-4 (1.1 mN/m) and LPI-pectin-3.5 (2.3 mN/m) after 1 s, indicating that LPI-4 and LPI-3.5 adsorb faster than LPI-pectin-4 and LPI-pectin-3.5. This can mainly be attributed to the larger

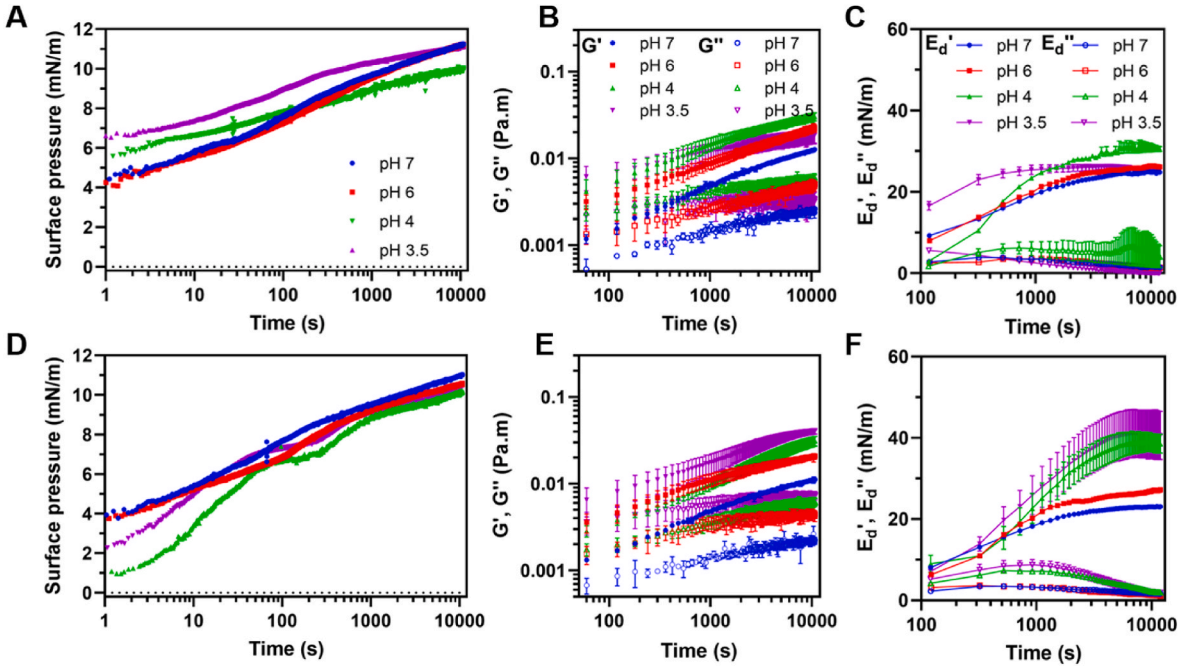

Fig. 1. Interfacial pressure of LPI (A) and LPI-pectin (D) as a function of time from 1 s to 10,800 s. Interfacial shear modulus (G′ and G″) (0.1 % and 0.1 Hz) and dilatational modulus (E_d' and E_d'') (3 % and 0.02 Hz) of the oil-water interface formed by LPI (B and C) and LPI-pectin mixtures (E and F) during the adsorption. The total biopolymer concentration of all samples is 0.1 wt%.

particle size (Fig. S1A and S1B) and lower surface hydrophobicity (Fig. S1D) of LPI-pectin-4 and LPI-pectin-3.5 compared to LPI-4 and LPI-3.5, which reduced the affinity of LPI-pectin complexes for the oil-water interface. At pH 7 and 6, LPI-pectin mixtures showed a comparable interfacial pressure after 1 s than LPI, which may indicate a comparable diffusion rate between LPI-pectin mixtures and LPI at pH 7 and 6. After 3 h of adsorption, LPI-pectin at pH 3.5–7 (except pH 6) showed a comparable equilibrium interfacial pressure (10.2–11.0 mN/m) to LPI at pH 3.5–7 (10.0–11.2 mN/m). These values were considerably lower than those observed at the air-water interface (LPI-pectin mixtures, 24.7–28.2 mN/m; LPI, 24.7–29.2 mN/m) (Ma et al., 2024a; Ma et al., 2025).

To monitor the development of the mechanical properties of the oil-water interfaces, we performed interfacial shear and dilatational time sweeps during 3 h of adsorption (Fig. 1B–C and 1E-F). In the initial adsorption period (i.e., the first point of the plot), LPI and LPI-pectin mixtures showed comparable G′ and E_d' values at pH 7 and pH 6. At pH 4, LPI-pectin complexes showed a larger E_d' value (8.97 ± 2.11 mN/m) than LPI (2.91 ± 0.12 mN/m), indicating that LPI-pectin-4 could form a stiffer oil-water interface at the early adsorption phase than LPI-4. While LPI-3.5 had a significantly higher E_d' value (16.59 ± 1.07 mN/m) than LPI-pectin-3.5 (7.09 ± 1.33 mN/m). As shown in Fig. S1D, LPI-3.5 had a markedly higher surface hydrophobicity (1.00 ± 0.01) than LPI-pectin-3.5 (0.41 ± 0.01). The higher surface hydrophobicity of LPI-3.5 may have resulted in a higher surface density and stronger in-plane hydrophobic interactions between proteins upon adsorption, which resulted in the formation of a stiffer oil-water interface in the early adsorption phase.

During adsorption, both LPI and LPI-pectin mixtures at pH 7 and 6 showed a gradual increase in the dilatational modulus up to 1000 s, and afterwards the modulus leveled off (Fig. 1C and F). Similar trends were also observed in LPI-pectin complexes at pH 4 and 3.5, but the transition point came later at around 6000 s. While the shear modulus of all samples continuously increased with time during adsorption without clear transition points (Fig. 1B and E). This could be because the value of 3 % for the strain of the dilatational rheology (Fig. 1C and F) was already in the non-linear regime, which could affect the formation of the interfacial microstructure. Choosing a strain below 3 % was not possible due to inaccuracy of the measurement at lower strains.

3.1.2. *Interfacial shear rheology*

After 3 h of adsorption, the oil-water interfaces of LPI and LPI-pectin were subjected to interfacial shear deformation in frequency sweeps (Fig. 2). All interfaces showed a higher elastic modulus (G′) than loss modulus (G″) (Fig. 2A and B), indicating the formation of solid-like interfaces in the applied frequency range. The change of elastic modulus with applied frequency was fitted with a power-law equation ($G' \sim \omega^n$) (Fig. 2B). All interfaces showed nearly frequency-independent behavior with n values between 0.10 and 0.15, indicating the formation of soft disordered solid-like oil-water interfaces with a wide spectrum of relaxation time.

We subsequently performed strain sweeps at strains from 0.1 % to 100 % and a fixed frequency of 0.1 Hz (Fig. 3). Both LPI and LPI-pectin showed constant G′ values before reaching critical strains, which represented the extent of the linear viscoelastic (LVE) regimes. In the LVE regimes, all interfaces showed larger G′ values than G″ values, indicating the formation of viscoelastic solid-like oil-water interfaces. The LPI-pectin-4 (34.1 ± 3.8 mPa m) and LPI-pectin-3.5 (41.8 ± 2.5 mPa m) had larger G′ values in the LVE regimes than LPI-4 (33.4 ± 3.6 mPa m) and LPI-3.5 (19.5 ± 3.6 mPa m), while the LPI-pectin-7 (12.5 ± 0.6 mPa m) and LPI-pectin-6 (22.5 ± 1.2 mPa m) had slightly lower G′ values than LPI-7 (14.3 ± 0.5 mPa m) and LPI-6 (25.8 ± 2.6 mPa m), indicating the electrostatic complexes could form stiffer oil-water interface than LPI at pH 4 and 3.5, while the co-soluble mixtures formed slightly weaker oil-water interfaces than LPI at pH 7 and 6. When the strains further increased beyond the LVE regimes, the G′ values started to decrease until a critical crossover-point, where the G′ started to be lower than G''. The LPI-pectin-4 (14.6 %) and LPI-pectin-3.5 (13.0 %) interfaces showed a markedly lower crossover-points than LPI-4 (40.5 %) and LPI-3.5 (56.9 %), while the LPI-pectin-7 (89.8 %) and LPI-pectin-6 (>100 %) showed comparable crossover-points as LPI-7 (>100 %) and LPI-6 (>100 %). These results indicated that both LPI and LPI-pectin mixtures at pH 7 and 6 showed similar solid-like behavior over a wide range of strains, while LPI-pectin complexes at pH 4 and 3.5 formed interfaces which were more brittle and yielded at lower strains. Additionally, LPI-pectin-4 and LPI-pectin-3.5 clearly showed slight overshoots of the G″ curves at strains of around 5.8 %, which is referred to as the "Payne effect", and is frequently observed in particle network systems (Hyun et al., 2002). While this type of behavior (also known as type III nonlinear behavior) was absent in LPI and LPI-pectin mixtures at pH 7 and 6, which indicated potentially different types of oil-water interfaces being formed by LPI or LPI-pectin mixtures at pH 7 and 6, and LPI-pectin complexes at pH 4 and 3.5. In our previous study on air-water interfaces (Ma et al., 2024b), no Payne effect was observed at the air-water interfaces stabilized by LPI-pectin-4 and LPI-pectin-3.5.

Normalized Lissajous plots were constructed to further analyze linear and non-linear viscoelastic behavior of LPI and LPI-pectin at different pH (Fig. 3E and F). In the LVE regimes (0.5 %), both LPI and LPI-pectin had Lissajous plots with narrow ellipse shapes with straight decomposed elastic components, indicating the dominance of elastic behavior. In the NLVE regime, at 16 % strain, the Lissajous plots for LPI at all pH values and LPI-pectin at pH 6 and 7 were still nearly ellipsoidal but became wider, indicating increased viscous dissipation. For LPI-pectin at pH 3.5 and 4 at 16 % deformation the plots already took on a rhomboidal shape

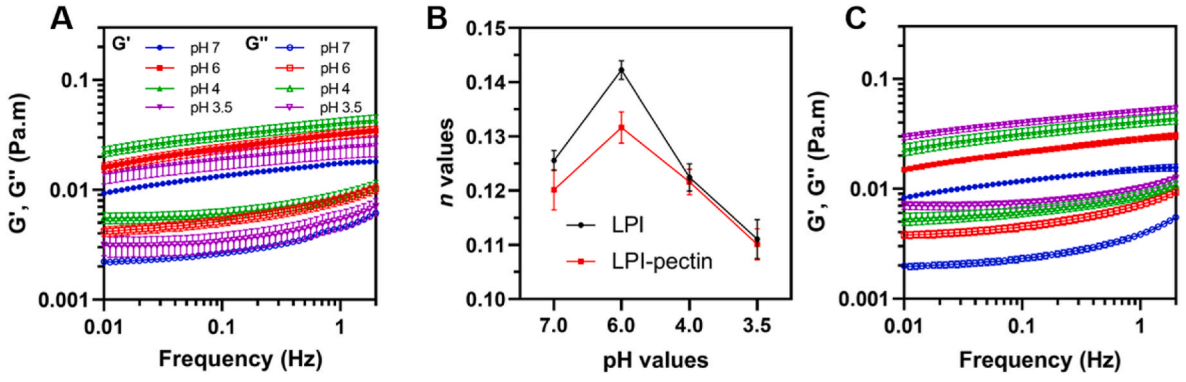

Fig. 2. Interfacial shear modulus (G′ and G″) of LPI (A) and LPI-pectin (C) at pH 3.5–7.0 as a function of frequency (0.01–2 Hz) and at a fixed strain of 1 %. (B) The power-law fitting exponent (n value) of LPI and LPI-pectin calculated from the interfacial shear frequency sweep in Fig. 2A and C. The total biopolymer concentration of all samples is 0.1 wt%.

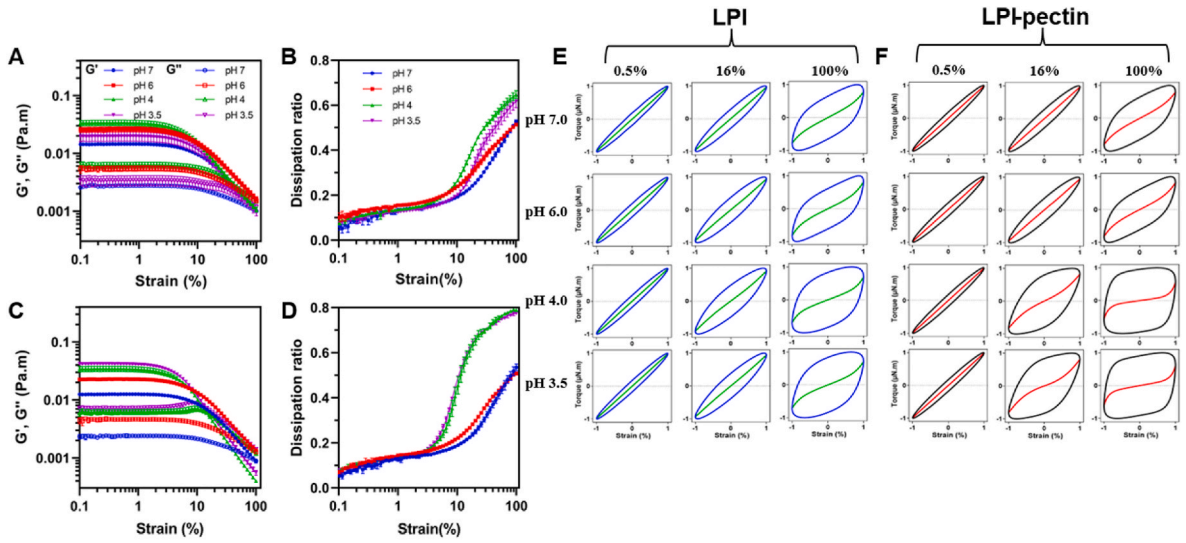

Fig. 3. Interfacial shear modulus (G′ and G″) of LPI (A) and LPI-pectin (C) as a function of strain (0.1–100 %) at pH 3.5–7.0. (E)(F) Normalized Lissajous plots (0.5 %, 16 %, and 100 %) of LPI and LPI-pectin at pH 7.0, pH 6.0, pH 4.0, and pH 3.5. The dissipation energy ratio of LPI (B) and LPI-pectin (D) at pH 3.5–7.0. The total biopolymer concentration of all samples is 0.1 wt%.

with inverse sigmoidal decomposed elastic components, indicating an increased viscous behavior due to significant disruption of the interfacial microstructure. At 100 % strain, for both LPI and LPI-pectin mixtures at pH 7 and 6 the plots also showed a rhomboidal shape, but the plots were narrower than those for LPI-pectin-4 and LPI-pectin-3.5, which had clearly more plastic behavior at 100 % strain with nearly zero slopes of the decomposed elastic component around zero intracycle strain, indicating the significant disruption of the interfacial microstructure at these large strains. To quantitatively analyze the Lissajous plots, we further calculated the dissipated energy ratio (φ) as shown in Fig. 3B and D. In the LVE regimes, both LPI and LPI-pectin showed φ values smaller than 0.2, indicating the dominance of elastic behavior in the LVE regime. As the strain increased, LPI and LPI-pectin mixtures at pH 7 and 6 reached a value around 0.5 at 100 % strain, suggesting there is still a significant contribution of residual elasticity to the response at these large shear deformations. In contrast, LPI and LPI-pectin complexes at pH 4 and 3.5 showed dramatically increased φ values to around 0.6 and 0.8 at 100 % strain, respectively, suggesting predominantly viscous behavior at these large shear deformations due to the disruption of the interfacial microstructure.

3.1.3. *Interfacial dilatational rheology*

The oil-water interfacial dilatational rheology of LPI and LPI-pectin at different pH was studied by performing dilatational frequency sweeps and amplitude sweeps (Fig. 4). In the frequency sweeps (Fig. 4B), both LPI and LPI-pectin showed power-law behavior ($E_d' \sim \omega^m$) with m values between 0.01 and 0.03, which were significantly lower than 0.5, indicating the low exchangeability of the stabilizers between bulk phase and the oil-water interface (Lucassen & Van Den Tempel, 1972). In the amplitude sweeps (Fig. 4A and C), the elastic modulus (E_d') of LPI-pectin complexes at pH 4 and pH 3.5 dramatically reduced from 37.5 to 40.7 mN/m at 3 % to 17.8–18.4 mN/m at 50 %, indicating the disruption of the interfacial microstructure at large deformations. While LPI and LPI-pectin mixtures at pH 7 and pH 6 showed less reduction of E_d' with increasing amplitude than the LPI-pectin complexes at pH 4 and 3.5. The E_d' of LPI-pectin-4 (37.5 ± 1.9 mN/m) and LPI-pectin-3.5 (40.7 ± 1.8 mN/m) at 3 % was also markedly larger than LPI-4 (29.1 ± 1.9 mN/m) and LPI-3.5 (23.9 ± 2.2 mN/m), while the E_d' of LPI-7/LPI-6 and LPI-pectin-7/LPI-pectin-6 at 3 % was not significantly different. This result suggested that LPI-pectin complexes at pH 4 and 3.5 formed stiffer oil-water interfaces than LPI at pH 4 and 3.5, while the LPI-pectin mixtures at pH 7 and 6 formed comparably stiff oil-water interfaces as LPI at pH 7 and 6. At an amplitude of 3 %, the E_d' of LPI at pH 4.0 (29.1

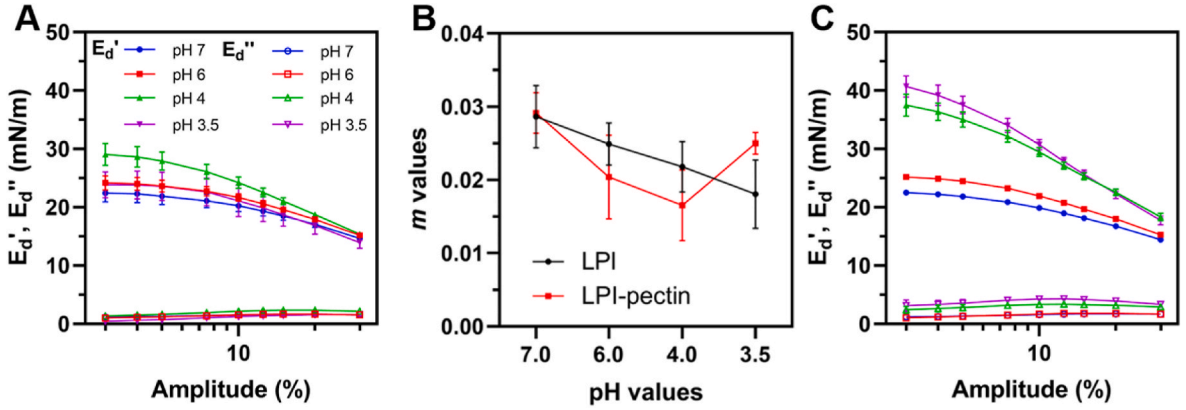

Fig. 4. Interfacial dilatational modulus (E_d' and E_d'') of LPI (A) and LPI-pectin (C) as a function of amplitude (%) at pH 3.5–7.0. (B) The power law exponent (*m* value) of LPI and LPI-pectin calculated from interfacial dilatational frequency sweeps (3 % and 0.02 Hz). The total biopolymer concentration of all samples is 0.1 wt%.

mN/m) was close to Rubisco (~32 mN/m) (Ma et al., 2025) and larger than lentil/faba/chickpea proteins (~19–23 mN/m) (Shen et al., 2025), suggesting that the potential of LPI in stabilizing oil-water interfaces.

We further constructed Lissajous plots (Fig. 5) to analyze the nonlinear behavior of LPI and LPI-pectin at pH 3.5–7.0. At 5 % deformation, all plots were narrow, implying a nearly fully elastic response. With increased amplitudes, those plots started to widen and became asymmetric in the extension and compression part, which could be seen most clearly in the plots at 30 % deformation. Upon extending the interfaces from −0.3 to +0.3, we first observed a steady increase in the slope of the plots, followed by a decrease in the slope (known as strain softening). Upon compression from +0.3 to −0.3, first a nearly linear reduction of interfaical pressure was observed, followed by a decrease in slope towards maximum compression, which would imply strain softening. The latter phenomenon could be the result of jamming of the interfacial structure, followed either by buckling of the interface or expulsion of material into the bulk phase. The total stress response at 30 % deformation includes contributions from network interactions and changes in surface density, which can be separated by the general stress decomposition (GSD) method (de Groot, Yang, & Sagis, 2023).

3.1.4. General stress decomposition (GSD)

Based on the general stress decomposition (GSD), the total stress response was split into odd harmonics and even harmonics. The odd harmonics are related to the change in the interfacial microstructure and consist of elastic (τ_1) and viscous (τ_2) components. The even harmonics represent the contributions to the surface stress response resulting from changes in surface density and also include both elastic (τ_4) and viscous (τ_3) components (de Groot, Sagis, & Yang, 2023). Examples of the decomposed plots of LPI and LPI-pectin are shown in Fig. S2. In the quantified GSD plots shown in Fig. 6, we defined five parameters, including $E_{\tau1}$, $E_{\tau4}$, $U_{d\tau2}$, $U_{d\tau3}$, and γ_s, according to de Groot, Yang, and Sagis (2023). $E_{\tau1}$ and $E_{\tau4}$ are two secant elastic moduli, which represent the interfacial network stiffness and resistance to surface density changes, respectively. $U_{d\tau2}$ and $U_{d\tau3}$ are two dissipated energy parameters associated with the disruption of the interfacial network and change of surface density, respectively. Additionally, γ_s describes the vertical shift of the τ_4 curve, which is related to how far the interfaces are driven out of equilibrium by the oscillations.

The $E_{\tau1}$ modulus of all interfaces reduced with increased amplitudes, implying the disruption of interfacial structure at large deformations (Fig. 6A and F). LPI-pectin-4 and LPI-pectin-3.5 showed markedly larger $E_{\tau1}$ modulus than LPI-4 and LPI-3.5 at small deformations, while LPI-pectin-7 and LPI-pectin-6 had similarly lower $E_{\tau1}$ modulus as LPI-7 and LPI-6. These results indicated that the electrostatic complexes formed at pH 4 and pH 3.5 were more efficient in improving the interfacial stiffness of LPI than the co-soluble mixtures at pH 7 and 6. Besides, LPI-pectin-4 and LPI-pectin-3.5 tended to have a higher dissipated energy of τ_2 ($U_{d\tau2}$) than LPI-4 and LPI-3.5 (Fig. 6D and I), indicating that the stiffer oil-water interfaces of LPI-pectin-4 and LPI-pectin-3.5 required more energy to be disrupted than those of LPI-4 and LPI-3.5.

The $E_{\tau4}$ modulus of all samples is significantly smaller than $E_{\tau1}$ which indicates that the odd harmonics dominate the response. LPI-pectin-4 and LPI-pectin-3.5 were positive over the range of amplitudes from 10 % to 30 %, while LPI-4 showed negative values of $E_{\tau4}$ modulus at those amplitudes (Fig. 6B and G). Most proteins or protein-polysaccharide complexes at air-water interfaces show a parabolic shape for τ_4 with a maximum at zero strain; this results in negative values for $E_{\tau4}$. Here most of the τ_4 curves are inverted, with a minimum at zero strain, except for LPI-4 and LPI-pectin-7. This behavior is typical for oil-water interfaces, and the result of the aforementioned strain softening towards maximum compression. With respect to the vertical shift (γ_s), LPI-4 displayed a more negative shift than LPI-pectin-4, while at all other pH values the LPI-pectin samples had a more negative shift than the LPI samples (Fig. 6C and H). In view of its lower charge and smaller size (compared to its complex) LPI-4 may have formed a denser layer, with lower mobility, and hence is driven further out of equilibrium by the oscillatory deformations. This would also be in line with the more negative value for $E_{\tau4}$ of this sample. All interfaces showed extremely low values of $U_{d\tau3}$ (less than 0.5 mJ/m^2) (Fig. 6E and J), indicating limited bulk-interface exchange at large deformations.

Overall, LPI-pectin-4 and LPI-pectin-3.5 formed the stiffest oil-water interfaces, while LPI-4 formed weaker but more densely packed oil-water interfaces. In contrast, LPI-pectin-7 and LPI-pectin-6 formed comparably weak oil-water interfaces as LPI-7 and LPI-6.

3.2. Emulsion properties

3.2.1. Emulsifying properties – droplet formation

In oil droplet formation during emulsification, proteins must initially attach to the newly created oil-water interface by both diffusion and convection, to prevent recoalescence of newly formed oil droplets (McClements, 2004; Perrier-Cornet et al., 2005). The efficiency of droplet formation is typically dominated by the following mechanisms: (1) electrostatic repulsion (related to the droplet charges), (2) steric repulsion (related to the interfacial thickness), and (3) mechanical properties of the oil-water interfaces (related to the interfacial stiffness) (Ma & Chatterton, 2021; Yang et al., 2024).

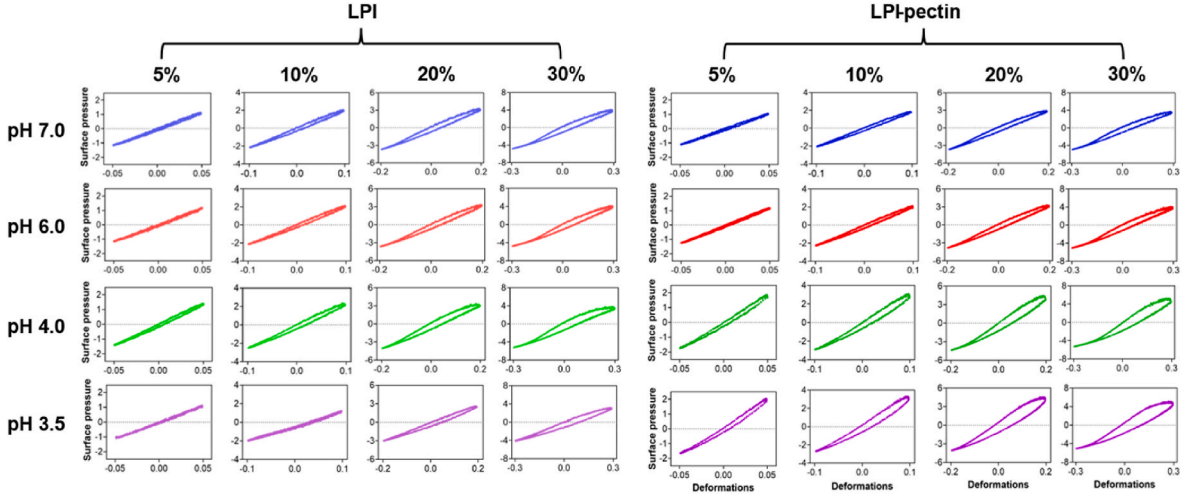

Fig. 5. Lissajous plots of LPI (left panel) and LPI-pectin (right panel) at amplitudes of 5 %, 10 %, 20 %, and 30 %. The total biopolymer concentration of all samples is 0.1 wt%.

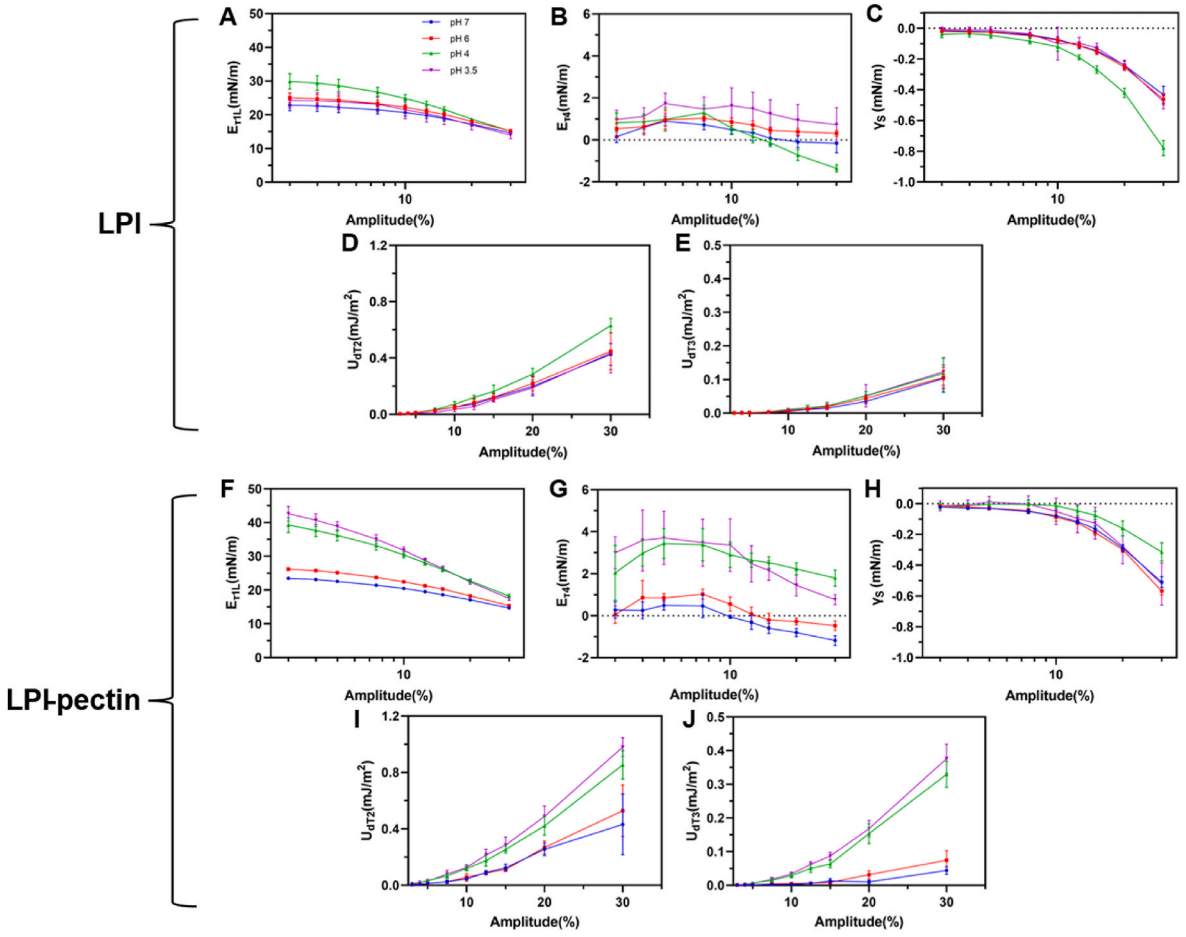

Fig. 6. The modulus of τ_1 (A and F) and τ_4 (B and G), the vertical shift of τ_4 (C and H), and the dissipation energy of τ_2 (D and I) and τ_3 (E and J) for LPI (A–E) and LPI-pectin (F–J) at pH 7.0, 6.0, 4.0, and 3.5. The total biopolymer concentration of all samples is 0.1 wt%.

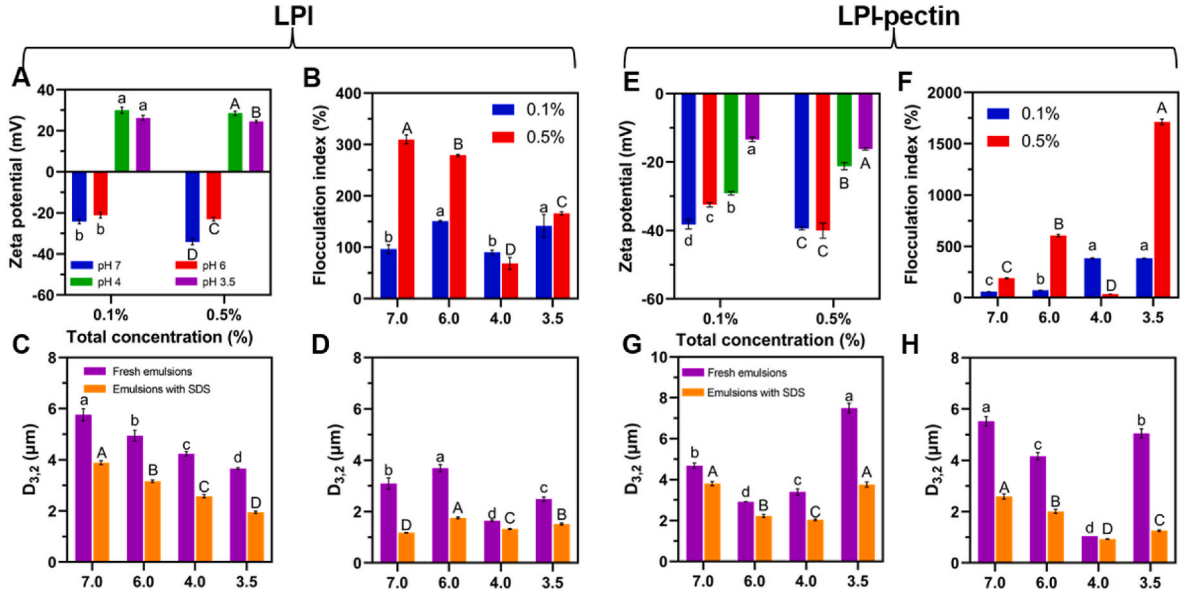

Fig. 7. Zeta potential (mV) (A and E), flocculation index (B and F) of the fresh emulsions, and surface-based average droplet size ($D_{3,2}$) of emulsions with 0.1 wt% total concentrations (C and G) and with 0.5 wt% total concentration (D and H) for LPI (A–D) and LPI-pectin (E–H) at pH 7.0, pH 6.0, pH 4.0, and pH 3.5. **Note**: the flocculation index (%) in Fig. 7B and F was calculated by: ($D_{4,3}$ of fresh emulsions - $D_{4,3}$ of emulsions in SDS)/$D_{4,3}$ of emulsions in SDS*100 %. Significant differences between samples were indicated by different letters (a-d or A-D).

Oil in water emulsions of LPI and LPI-pectin at pH 3.5–7 were prepared at total biopolymer concentrations of 0.1 wt% and 0.5 wt%. In Fig. S3, the fresh emulsions stabilized with 0.1 wt% LPI and LPI-pectin at pH 3.5–7 showed bimodal distributions, in which all those samples had a small peak at a droplet size around or slightly below 1 μm, and a second peak around 10–25 μm. To further check for droplet flocculation of the fresh emulsions, 1 wt% of SDS was added to the emulsions, which could adsorb to the oil-water interfaces and cause electrostatic repulsion to break up any flocculated droplets and hence enable the measurement of the size of single oil droplets (Dickinson, 2019). After adding 1 wt% SDS, the droplet size distributions of all samples were clearly shifting to smaller droplet size (Fig. S3), implying that extensive droplet flocculation had occurred at this lower biopolymer concentration. The surface-based average droplet size ($D_{3,2}$) of LPI and LPI-pectin at 0.1 wt % were reduced from 3.7-5.8 μm to 2.0–3.9 μm and from 2.9-7.5 μm to 2.0–3.8 μm after adding 1 wt% SDS (Fig. 7). LPI and LPI-pectin had a flocculation index (FI) ranging from 90 % to 151 % and from 59 % to 385 % (Fig. 7), respectively, which is consistent with the microscopic images in Figs. S3 and S4.

With the total biopolymer concentration increased to 0.5 wt%, all samples except LPI-pectin-4 still exhibited multimodal distributions, and curves still shifted to smaller sizes after adding 1 wt% SDS (except LPI-4), implying oil droplet flocculation occurred even at higher concentrations (Fig. 7). This high degree of flocculation in the emulsion stabilized by protein-polysaccharide mixtures was also reported by many other studies, such as whey protein-xanthan mixtures (Euston et al., 2002), soy protein-pectin mixtures (Roudsari et al., 2006), and whey proteins and soluble soybean polysaccharides mixtures (Ray & Rousseau, 2013). The higher degree of flocculation in LPI-7/LPI-6 and LPI-pectin-7/LPI-pectin-6 stabilized emulsions might be attributed to large non-adsorbed protein aggregates (Fig. S1A) and non-adsorbed pectin (due to the co-solubilization of LPI and pectin at pH 7 and 6), respectively, which may induce depletion flocculation of the oil droplets (Blijdenstein et al., 2004; Dickinson & Golding, 1997). LPI-pectin-4 stabilized emulsions also showed a lower degree of flocculation compared to LPI-pectin-3.5, due to slightly higher charges of the droplets of the former emulsions (Fig. 7), which could provide more electrostatic repulsion. Additionally, the different particle size distributions between LPI-pectin-3.5 and LPI-pectin-4 could also cause the aforementioned emulsion flocculation. As shown in Fig. S1B, LPI-pectin-4 showed a bimodal distribution, indicating the coexistence of both small protein clusters (~59.1 nm) and large complexes (~267.2 nm), while LPI-pectin-3.5 showed a monomodal distribution, indicating the samples mostly contained large complexes (~310.7 nm). The overall smaller size of LPI-pectin-4 could provide better surface coverage (i.e., more complexes adsorbed at the oil droplet). As the increased concentrations from 0.1 wt% to 0.5 wt%, more LPI-pectin-4 complexes could adsorb to the oil droplets and significantly reduce the bridge flocculation between oil droplets at 0.5 wt%. In contrast, the large size of LPI-pectin-3.5 reduced the surface coverage and resulted in less complex adsorption to the oil droplets than LPI-pectin-4. At the concentration of 0.5 wt%, the excessive amount of non-adsorbed LPI-pectin-3.5 complexes in the continuous phase could induce severe depletion flocculation of the oil droplets.

To reduce the flocculation of the emulsions stabilized with protein-pectin mixtures, several strategies can be considered according to the results presented in this study: (1) avoid the pH ranges (close to neutral pH) where proteins and pectin were co-solubilized in the continuous phases; (2) choose right pH ranges where the protein-pectin complexes carry enough charges to increase the interdroplet electrostatic repulsion; (3) choose right protein to pectin ratio to increase the size of complexes, thereby increasing interfacial thickness of interfacial layer. However, the results presented in this study only focus on the lupin protein-pectin mixtures at pH 3.5–7.0, the results may not be generalizable to other protein-polysaccharide mixtures.

The single droplet sizes ($D_{3,2}$ after adding 1 wt% SDS) of LPI-pectin-4 (0.93 ± 0.01 μm) and LPI-pectin-3.5 (1.26 ± 0.03 μm) at 0.5 wt% were slightly smaller than those of LPI-4 (1.32 ± 0.02 μm) and LPI-3.5 (1.52 ± 0.04 μm). While LPI-pectin-7 (2.59 ± 0.10 μm) and LPI-pectin-6 (2.01 ± 0.08 μm) were slightly larger than LPI-7 (1.18 ± 0.01 μm) and LPI-6 (1.76 ± 0.03 μm). Those results indicated that the LPI-pectin complexes at pH 4 and 3.5 clearly showed better emulsifying properties than LPI at pH 4 and 3.5, while LPI-pectin mixtures at pH 7 and 6 had worse emulsifying properties than LPI at pH 7 and 6. This could be attributed to the stiffer oil-water interfaces of LPI-pectin-4 and LPI-pectin-3.5, which may reduce droplet re-coalescence during the emulsification process. It should be noticed that the emulsions stabilized with LPI-pectin at pH 3.5–7 (especially at 0.5 wt%) clearly showed less creaming than LPI at pH 3.5–7 (Fig. S6) after 7 days of storage, indicating the improved emulsion creaming stability by adding pectin, most likely resulting from a higher viscosity of the continuous phase.

3.2.2. *Emulsion flow stability*

The emulsions stabilized with 0.5 wt% LPI and LPI-pectin at pH 3.5–7 were further subjected to deformation by mixing with an Ultra-Turrax (at speeds from 5000 rpm to 15000 rpm) to test the emulsion stability in large deformations, which induce large shear and dilatational deformations of the surface of the oil droplets. For LPI, after mixing treatment, all samples showed several clear new peaks with increased droplet sizes, which were more visible at the higher speed of 15000 rpm (Fig. 8H-K). In comparison, LPI-pectin-4 and LPI-pectin-3.5 clearly showed fewer peak changes (i.e., lower new peak volume percentages after treatment) than LPI-4 and LPI-3.5, while LPI-pectin-7 and LPI-pectin-6 appeared to have comparable peak changes as LPI-7 and LPI-6 (Fig. 8A-D). The volume changes of the new peaks after high shear treatment relative to the original peak before treatment were then calculated to quantitatively indicate the stability of emulsions under high mixing treatment. As shown in Fig. 8E–G and 8L-N, LPI-pectin complexes at pH 3.5 and 4 had smaller volume changes than LPI at pH 3.5 and 4. These results indicated that the emulsions stabilized with LPI-pectin complexes at pH 3.5 and 4 had markedly higher stability than those stabilized with LPI at pH 3.5 and 4, while the emulsions stabilized with LPI-pectin mixtures and LPI at pH 7 and 6 showed comparable instability against high flow rates. Those observations aligned well with the interfacial rheology results, where the stiffer oil-water interfaces of LPI-pectin-4 and LPI-pectin-3.5 gave better emulsion stability than LPI-4 and LPI-3.5, while the weaker interfaces of LPI and LPI-pectin mixtures at pH 7 and 6 formed emulsions that were unstable against high flow rates.

4. Conclusions

This study systematically investigated the oil-water interfacial properties and emulsifying properties of lupin protein and lupin protein-pectin mixtures at acidic pH (3.5 and 4.0) and pH close to neutral conditions (6 and 7). Our results showed that LPI-pectin complexes at pH 3.5 and 4.0 had better interfacial and emulsifying properties than LPI-pectin co-solubilized mixtures at pH 6.0 and 7.0. By using new methodologies, i.e., large amplitude oscillatory shear (LAOS), large amplitude oscillatory dilatation (LAOD), and general stress decomposition (GSD), we found that the LPI-pectin mixtures at different pH showed completely different oil-water interfacial properties. These different interfacial properties resulted in different emulsion stability under flow conditions. At pH 7 and 6, the LPI-pectin co-solubilized mixtures showed a comparable adsorption rate to the oil-water interfaces as LPI at pH 7 and 6, and finally developed comparably weak oil-water interfaces. This indicates that at these pH values, it is mostly the protein that adsorbs at the interface, while the pectin remains in solution. The LPI-pectin complexes at pH 4 and 3.5 adsorbed slower to the oil-water interface than LPI at pH 4 and 3.5, due to the larger particle size of the complexes. The LPI-pectin complexes at pH 4 and 3.5 formed stiffer oil-water interfaces than LPI at pH 4 and 3.5. The stiffer oil-water

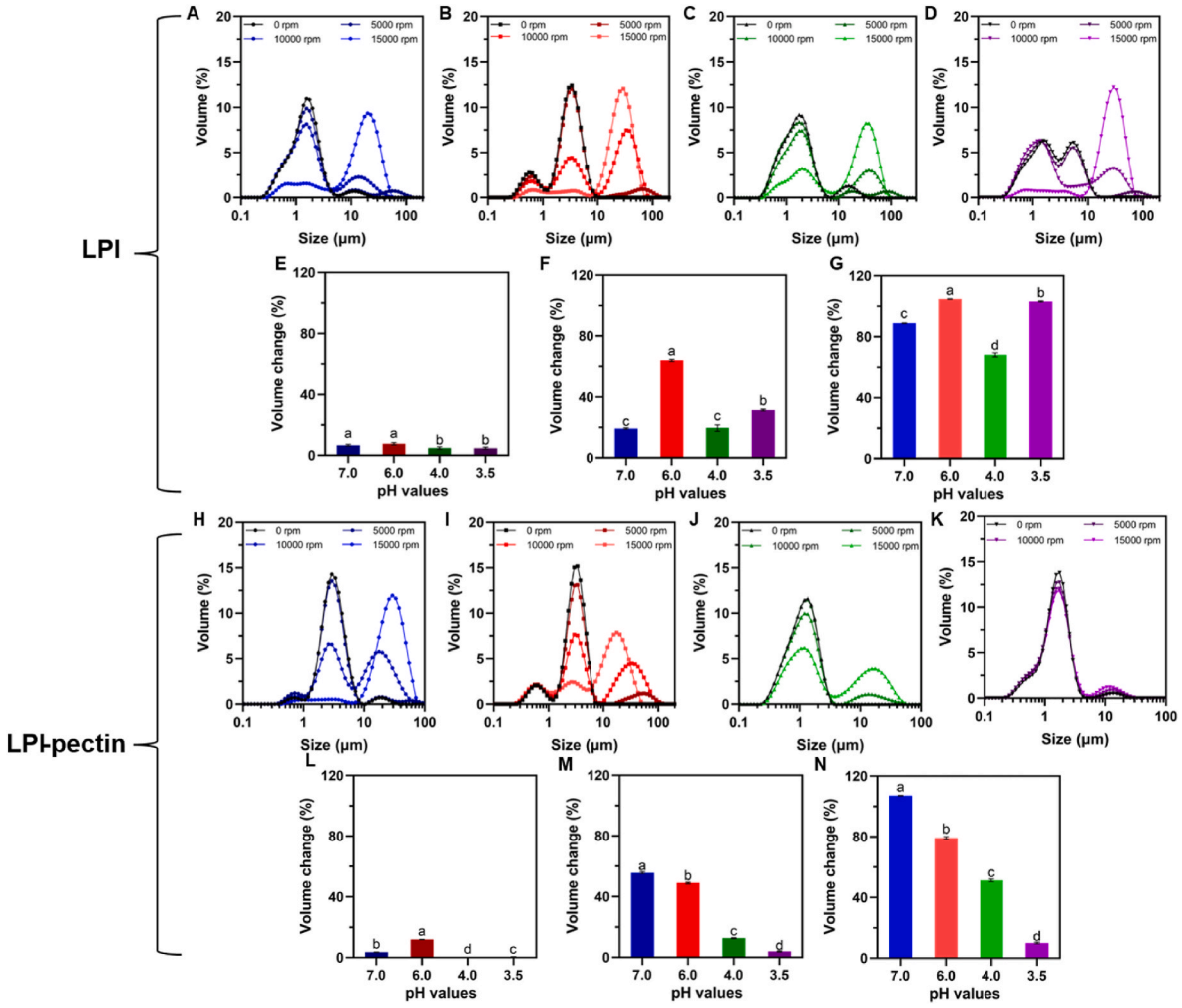

Fig. 8. Shear stability tests for LPI (A–G) and LPI-pectin (H–N) at pH 7.0 (A and H), pH 6.0 (B and I), pH 4.0 (C and J), and pH 3.5 (D and K). Volume changes (%) from droplet size distributions (A-D and H-K) before shear tests (0 rpm) and after 5000 rpm (E and L), 10000 rpm (F and M), and 15000 rpm (G and N) shear tests for LPI and LPI-pectin mixtures at pH 7.0, pH 6.0, pH 4.0, and pH 3.5. Significant differences between samples were indicated by different letters (a-d or A-D). The total biopolymer concentration of all samples is prepared at 0.5 wt%.

interfaces of LPI-pectin-4 and LPI-pectin-3.5 could explain their better emulsifying properties and emulsion flow stability at 0.5 wt% than LPI-4 and LPI-3.5. However, LPI-pectin-3.5 showed a markedly higher degree of emulsion flocculation (flocculation index = 1713 % at 0.5 wt%) than LPI-pectin-4 (flocculation index = 35 % at 0.5 wt%), due to its lower charge and non-adsorbed complexes at high concentrations. Both LPI and LPI-pectin co-solubilized mixtures at pH 7 and 6 showed large degrees of droplet flocculation (especially at 0.5 wt%), most likely due to depletion flocculation as a result of non-adsorbed proteins or pectin. Additionally, the weaker oil-water interfaces of LPI and LPI-pectin mixtures at pH 7 and 6 also resulted in unstable emulsions against flow-induced droplet coalescence.

Overall, LPI-pectin complexes at pH 4 showed better interfacial and emulsifying properties than LPI at pH 4. Although the LPI-pectin complexes at pH 3.5 improved the interfacial properties of proteins, the reduced charges induced large degrees of emulsion flocculation, which is undesired in food applications. At pH 7 and 6, the addition of pectin to LPI can neither improve interfacial properties nor emulsifying properties. Considering the low solubility of pure LPI at pH 4, the addition of pectin could significantly improve protein solubility and also improve protein interfacial and emulsifying properties, making LPI more suitable for potential use in acid food products. Since other plant-based proteins also suffer from low solubility at acidic pH, this study could guide the food industry in choosing optimum conditions to use plant-based protein and polysaccharide mixtures to stabilize food emulsion systems. As the implications of polysaccharides to proteins may cause severe emulsion flocculation, food manufacturers should consider some useful strategies to reduce emulsion flocculation (such as avoiding the pH ranges close to neutral pH, increasing the charge density of protein-polysaccharide mixtures, and increasing the size of protein-polysaccharide mixtures by choosing appropriate mixing ratios).

CRediT authorship contribution statement

Xingfa Ma: Writing – original draft, Visualization, Validation, Methodology, Investigation, Conceptualization. **Mehdi Habibi:** Writing – review & editing, Supervision, Methodology, Conceptualization. **Leonard M.C. Sagis:** Writing – review & editing, Supervision, Methodology, Conceptualization.

Declaration of competing interest

The authors have declared that no competing interest exists.

Acknowledgements

X. Ma acknowledges the funding from China Scholarship Council (CSC NO. 202207940007).

Appendix A. Supplementary data

Supplementary data to this article can be found online at https://doi.org/10.1016/j.foodhyd.2025.111467.

Data availability

Data will be made available on request.

References

Albe-Slabi, S., Mesieres, O., Mathé, C., Ndiaye, M., Galet, O., & Kapel, R. (2022). Combined effect of extraction and purification conditions on yield, composition and functional and structural properties of lupin proteins. *Foods, 11*(11), 1646.

Arnoldi, A., Boschin, G., Zanoni, C., & Lammi, C. (2015). The health benefits of sweet lupin seed flours and isolated proteins. *Journal of Functional Foods, 18*, 550–563.

Bähr, M., Fechner, A., Hasenkopf, K., Mittermaier, S., & Jahreis, G. (2014). Chemical composition of dehulled seeds of selected lupin cultivars in comparison to pea and soya bean. *LWT–Food Science and Technology, 59*(1), 587–590.

Blijdenstein, T., Zoet, F., Van Vliet, T., Van der Linden, E., & Van Aken, G. (2004). Dextran-induced depletion flocculation in oil-in-water emulsions in the presence of sucrose. *Food Hydrocolloids, 18*(5), 857–863.

Boukid, F., & Pasqualone, A. (2022). Lupine (Lupinus spp.) proteins: Characteristics, safety and food applications. *European Food Research and Technology, 248*(2), 345–356.

Chin, Y. Y., Chew, L. Y., Toh, G. T., Salampessy, J., Azlan, A., & Ismail, A. (2019). Nutritional composition and angiotensin converting enzyme inhibitory activity of blue lupin (Lupinus angustifolius). *Food Bioscience, 31*, Article 100401.

Chukwuejim, S., & Aluko, R. E. (2024). Comparative study of the emulsifying properties of blue lupin, white lupin, and soybean protein isolates. *Lebensmittel-Wissenschaft und -Technologie, 206*, Article 116544.

Dalev, P. G., & Simeonova, L. S. (1995). Emulsifying properties of protein–pectin complexes and their use in oil-containing foodstuffs. *Journal of the Science of Food and Agriculture, 68*(2), 203–206.

de Groot, A., Sagis, L. M., & Yang, J. (2023). White asparagus stem proteins, from waste to interface stabilizer in food foams. *Food Hydrocolloids*, Article 109218.

de Groot, A., Yang, J., & Sagis, L. M. (2023). Surface stress decomposition in large amplitude oscillatory interfacial dilatation of complex interfaces. *Journal of Colloid and Interface Science, 638*, 569–581.

Dickinson, E. (2019). Strategies to control and inhibit the flocculation of protein-stabilized oil-in-water emulsions. *Food Hydrocolloids, 96*, 209–223.

Dickinson, E., & Golding, M. (1997). Depletion flocculation of emulsions containing unadsorbed sodium caseinate. *Food Hydrocolloids, 11*(1), 13–18.

Doxastakis, G., Papageorgiou, M., Mandalou, D., Irakli, M., Papalamprou, E., D'Agostina, A., et al. (2007). Technological properties and non-enzymatic browning of white lupin protein enriched spaghetti. *Food Chemistry, 101*(1), 57–64.

Drakos, A., Doxastakis, G., & Kiosseoglou, V. (2007). Functional effects of lupin proteins in comminuted meat and emulsion gels. *Food Chemistry, 100*(2), 650–655.

Duranti, M., Consonni, A., Magni, C., Sessa, F., & Scarafoni, A. (2008). The major proteins of lupin seed: Characterisation and molecular properties for use as functional and nutraceutical ingredients. *Trends in Food Science & Technology, 19*(12), 624–633.

Euston, S. R., Finnigan, S. R., & Hirst, R. L. (2002). Kinetics of droplet aggregation in heated whey protein-stabilized emulsions: Effect of polysaccharides. *Food Hydrocolloids, 16*(5), 499–505.

Ewoldt, R. H., Hosoi, A. E., & McKinley, G. H. (2008). New measures for characterizing nonlinear viscoelasticity in large amplitude oscillatory shear. *Journal of Rheology, 52*(6), 1427–1458.

Gharsallaoui, A., Yamauchi, K., Chambin, O., Cases, E., & Saurel, R. (2010). Effect of high methoxyl pectin on pea protein in aqueous solution and at oil/water interface. *Carbohydrate Polymers, 80*(3), 817–827.

Girard, M., Turgeon, S., & Paquin, P. (2002). Emulsifying properties of whey protein-carboxymethylcellulose complexes. *Journal of Food Science, 67*(1), 113–119.

Hickisch, A., Beer, R., Vogel, R. F., & Toelstede, S. (2016). Influence of lupin-based milk alternative heat treatment and exopolysaccharide-producing lactic acid bacteria on the physical characteristics of lupin-based yogurt alternatives. *Food Research International, 84*, 180–188.

Hyun, K., Kim, S. H., Ahn, K. H., & Lee, S. J. (2002). Large amplitude oscillatory shear as a way to classify the complex fluids. *Journal of Non-newtonian Fluid Mechanics, 107*(1–3), 51–65.

Jayasena, V., Chih, H. J., & Nasar-Abbas, S. (2010). Functional properties of sweet lupin protein isolated and tested at various pH levels. *Research Journal of Agriculture and Biological Sciences, 6*(2), 130–137.

Kato, A., Sato, T., & Kobayashi, K. (1989). Emulsifying properties of protein–polysaccharide complexes and hybrids. *Agricultural and biological chemistry, 53*(8), 2147–2152.

Li, W. W., Zhao, H. B., He, Z. Y., Zeng, M. M., Qin, F., & Chen, J. (2016). Modification of soy protein hydrolysates by Maillard reaction: Effects of carbohydrate chain length on structural and interfacial properties. *Colloids and Surfaces B-Biointerfaces, 138*, 70–77.

Lopes-da-Silva, J. A., & Monteiro, S. R. (2019). Gelling and emulsifying properties of soy protein hydrolysates in the presence of a neutral polysaccharide. *Food Chemistry, 294*, 216–223.

Lucassen, J., & Van Den Tempel, M. (1972). Dynamic measurements of dilational properties of a liquid interface. *Chemical Engineering Science, 27*(6), 1283–1291.

Ma, X., & Chatterton, D. E. (2021). Strategies to improve the physical stability of sodium caseinate stabilized emulsions: A literature review. *Food Hydrocolloids, 119*, Article 106853.

Ma, X., Habibi, M., Landman, J., Sagis, L. M., & Shen, P. (2025). Rubisco at interfaces II: Structural reassembly enhances oil-water interface and emulsion stabilization. *Food Hydrocolloids, 160*, Article 110820.

Ma, X., Habibi, M., & Sagis, L. M. (2024a). Interfacial and foaming properties of soluble lupin protein isolates: Effect of pH. *Food Hydrocolloids*, Article 110228.

Ma, X., Habibi, M., & Sagis, L. M. (2024b). pH-induced conformational changes of lupin protein-pectin mixtures and its effect on air-water interfacial properties and foaming functionality. *Food Hydrocolloids*, Article 110567.

McClements, D. J. (2004). Protein-stabilized emulsions. *Current Opinion in Colloid & Interface Science, 9*(5), 305–313.

Melo, T. S., Ferreira, R. B., & Teixeira, A. N. (1994). The seed storage proteins from Lupinus albus. *Phytochemistry, 37*(3), 641–648.

Mota, J., Lima, A., Ferreira, R. B., & Raymundo, A. (2020). Lupin seed protein extract can efficiently enrich the physical properties of cookies prepared with alternative flours. *Foods, 9*(8), 1064.

Muranyi, I. S., Volke, D., Hoffmann, R., Eisner, P., Herfellner, T., Brunnbauer, M., et al. (2016). Protein distribution in lupin protein isolates from Lupinus angustifolius L. prepared by various isolation techniques. *Food Chemistry, 207*, 6–15.

Niu, H., Chen, X., Fu, X., Zhang, B., Dou, Z., & Huang, Q. (2025). Pectin-stabilized emulsions: Structure-emulsification relationships, covalent and non-covalent modifications, and future trends. *Trends in Food Science & Technology*, Article 104986.

Opazo-Navarrete, M., Burgos-Díaz, C., Garrido-Miranda, K. A., & Acuña-Nelson, S. (2022). Effect of enzymatic hydrolysis on solubility and emulsifying properties of Lupin proteins (Lupinus luteus). *Colloids and Interfaces, 6*(4), 82.

Paraskevopoulou, A., Provatidou, E., Tsotsiou, D., & Kiosseoglou, V. (2010). Dough rheology and baking performance of wheat flour–lupin protein isolate blends. *Food Research International, 43*(4), 1009–1016.

Perrier-Cornet, J., Marie, P., & Gervais, P. (2005). Comparison of emulsification efficiency of protein-stabilized oil-in-water emulsions using jet, high pressure and colloid mill homogenization. *Journal of Food Engineering, 66*(2), 211–217.

Ray, M., & Rousseau, D. (2013). Stabilization of oil-in-water emulsions using mixtures of denatured soy whey proteins and soluble soybean polysaccharides. *Food Research International, 52*(1), 298–307.

Raymundo, A., Sousa, I., & Empis, J. (2000). EFFECT OF pH AND NaCI ON RHEOLOGICAL AND TEXTURAL PROPERTIES OF LUPIN PROTEIN EMULSIONS. In *Gums and stabilisers for the food industry* (Vol. 10, pp. 350–365). Elsevier.

Roudsari, M., Nakamura, A., Smith, A., & Corredig, M. (2006). Stabilizing behavior of soy soluble polysaccharide or high methoxyl pectin in soy protein isolate emulsions at low pH. *Journal of Agricultural and Food Chemistry, 54*(4), 1434–1441.

Shen, P., Twilt, F., Deng, B., Peng, J., Schroen, K., Sagis, L. M., et al. (2025). Oil-water interface and emulsion stabilization by pulse proteins. *Food Hydrocolloids*, Article 111093.

Shrestha, S., van't Hag, L., Haritos, V. S., & Dhital, S. (2021). Lupin proteins: Structure, isolation and application. *Trends in Food Science & Technology, 116*, 928–939.

Sujak, A., Kotlarz, A., & Strobel, W. (2006). Compositional and nutritional evaluation of several lupin seeds. *Food Chemistry, 98*(4), 711–719.

Van de Noort, M. (2024). Lupin: An important protein and nutrient source. In *Sustainable protein sources* (pp. 219–239). Elsevier.

Wang, Y., Ghosh, S., & Nickerson, M. T. (2019). Effect of pH on the formation of electrostatic complexes between lentil protein isolate and a range of anionic polysaccharides, and their resulting emulsifying properties. *Food Chemistry, 298*, Article 125023.

Wang, S. N., Yang, J. J., Shao, G. Q., Qu, D. N., Zhao, H. K., Yang, L. N., et al. (2020). Soy protein isolated-soy hull polysaccharides stabilized O/W emulsion: Effect of polysaccharides concentration on the storage stability and interfacial rheological properties. *Food Hydrocolloids, 101*.

Yang, J., Shen, P., de Groot, A., Mocking-Bode, H. C., Nikiforidis, C. V., & Sagis, L. M. (2024). Oil-water interface and emulsion stabilising properties of rapeseed proteins napin and cruciferin studied by nonlinear surface rheology. *Journal of Colloid and Interface Science, 662*, 192–207.

Yang, Y., & Xiang, D. (2022). Effect of coconut protein and xanthan gum, soybean polysaccharide and gelatin interactions in oil-water interface. *Molecules, 27*(9).

Zhang, X. Z., Luo, X. G., Wang, Y. X., Li, Y., Li, B., & Liu, S. L. (2020). Concentrated O/W Pickering emulsions stabilized by soy protein/cellulose nanofibrils: Influence of pH on the emulsification performance. *Food Hydrocolloids, 108*.

Zhao, H., Wang, S., Zhao, G., Li, Y., Liu, X., Yang, L., et al. (2022). Fabrication and emulsifying properties of non-covalent complexes between soy protein isolate fibrils and soy soluble polysaccharides. *Food & Function, 13*(1), 386–397.